

## MRI of the lung gas-space at very low-field using hyperpolarized noble gases

Arvind K. Venkatesh<sup>a,b</sup>, Adelaide X. Zhang<sup>a,c</sup>, Joey Mansour<sup>a,b</sup>, Lyubov Kubatina<sup>a</sup>, Chang-Hyun Oh<sup>d</sup>, Gregory Blasche<sup>e</sup>, M. Selim Ünlü<sup>f</sup>, Dilip Balamore<sup>g</sup>, Ferenc A. Jolesz<sup>a</sup>, Bennett B. Goldberg<sup>e,f</sup>, Mitchell S. Albert<sup>a,\*</sup>

<sup>a</sup>Department of Radiology, Brigham and Women's Hospital and Harvard Medical School, Boston, MA 02115, USA

<sup>b</sup>Department of Biomedical Engineering, Boston University, Boston, MA 02215, USA

<sup>c</sup>Department of Electrical Engineering, Massachusetts Institute of Technology, Cambridge, MA 02139, USA

<sup>d</sup>Department of Electronics and Information Engineering, Korea University, Seoul, South Korea

<sup>e</sup>Department of Physics, Boston University, Boston, MA 02215, USA

<sup>f</sup>Department of Electrical and Computer Engineering, Boston University, Boston, MA 02215, USA

<sup>g</sup>Department of Engineering/Physics/Technology, Nassau Community College, Garden City, NY 11530, USA

Received 14 February 2003; received in revised form 19 April 2003; accepted 20 April 2003

### Abstract

In hyperpolarized (HP) noble-gas magnetic resonance imaging, large nuclear spin polarizations, about 100,000 times that ordinarily obtainable at thermal equilibrium, are created in <sup>3</sup>He and <sup>129</sup>Xe. The enhanced signal that results can be employed in high-resolution MRI studies of void spaces such as in the lungs. In HP gas MRI the signal-to-noise ratio (SNR) depends only weakly on the static magnetic field (B<sub>0</sub>), making very low-field (VLF) MRI possible; indeed, it is possible to contemplate portable MRI using light-weight solenoids or permanent magnets. This article reports the first *in vivo* VLF MR images of the lungs in humans and in rats, obtained at a field of only 15 millitesla (150 Gauss). © 2003 Elsevier Inc. All rights reserved.

**Keywords:** Hyperpolarized; Helium; Xenon; Very low-field; MRI

### 1. Introduction

The promise of using hyperpolarized (HP) noble-gas magnetic resonance imaging [1] for human subjects is gradually being realized [2–6]. HP gas MRI with <sup>3</sup>He is currently being tested diagnostically in patients with chronic obstructive pulmonary disease (COPD), to stage the progress of therapeutic approaches to cystic fibrosis and asthma, and to screen patients and assess the outcome of lung volume reduction surgery in patients with emphysema and in patients undergoing lung transplantation [2–6]. In HP gas MRI, spin-exchange optical pumping [7] creates large non-equilibrium nuclear spin polarizations in <sup>3</sup>He and <sup>129</sup>Xe, as much as 100,000 times greater than that obtainable at thermal equilibrium. The enhanced signal facilitates high-

resolution MRI studies of void spaces such as in the lungs and sinuses. In addition, the solubility of <sup>129</sup>Xe makes it possible to image the blood vasculature, and tissues in the lung, heart and brain [1,8–12]. A special feature of HP gas MRI is that the signal-to-noise ratio (SNR) does not decrease appreciably when the static magnetic field (B<sub>0</sub>) is lowered [13–16], obviating the need for the ubiquitous heavy and expensive superconducting magnets in conventional thermal-equilibrium MRI. Portable MRI would then become feasible, using far smaller and cheaper resistive solenoids or suitably configured permanent magnets. This paper reports the first *in vivo* very low-field (VLF) MR images of the lung gas-space in humans and in rats breathing hyperpolarized <sup>3</sup>He and <sup>129</sup>Xe, obtained at a field of 15 millitesla (150 Gauss).

Dispensing with expensive high-field superconducting magnets should drastically reduce the cost of implementing HP gas MRI as a diagnostic modality for the detection and staging of lung diseases. HP gas MRI at VLF could become

\* Corresponding author. Tel.: +1-617-278-0621; fax: +1-617-278-0610.

E-mail address: malbert@bwh.harvard.edu (M.S. Albert).

portable, allowing the investigation of lung structure and function in a variety of settings, such as van-based imagers that could take this technique to patients unable to travel to a hospital, or even in the microgravity environments of spacecraft and space-stations.

## 2. Methods

**Very low-field MRI system.** Hyperpolarized  $^3\text{He}$  and  $^{129}\text{Xe}$  images were acquired on a 60 cm diameter prototype superconducting magnet with the magnetic field ramped down from 1.5 T to 15 mT (150 Gauss). Techron (Elkhart, IN, USA) 8604 gradient amplifiers were used to drive the x, y, and z gradients (maximum strength 0.8 Gauss/cm). The magnet and gradients were interfaced to a Resonance Instruments (Witney, UK) Maran Ultra imaging spectrometer. The Larmor resonance frequencies for  $^3\text{He}$  and  $^{129}\text{Xe}$  at 15 mT were 483.6 kHz and 175.6 kHz, respectively. To reduce electrostatic noise, a shield made from 0.1 mm thick copper sheet was installed within the magnet bore.

**Noble gas polarization.**  $^3\text{He}$  or  $^{129}\text{Xe}$  was polarized to about 5% via collisional spin-exchange with rubidium, optically pumped using an Optopower (Tucson, AZ, USA) 120 W fiber coupled laser-diode array.

**Animal preparation.** Sprague Dawley rats were anesthetized with a mixture of ketamine and xylazine. A 14-gauge catheter was inserted into the trachea, and silk ligatures were tied around the endotracheal tube. The animal was placed supine in the RF coil. The endotracheal breathing tube was connected to the gas delivery system. A polarized-gas delivery system [27], designed for accurate delivery of hyperpolarized gas inside an MR imager, was used for the animal experiments. All animal procedures were approved by the Harvard Medical Area Standing Committee on Animals.

**Animal imaging.** Solenoid RF coils, tuned to 483.6 kHz and 175.6 kHz, the Larmor resonance frequencies of  $^3\text{He}$  and  $^{129}\text{Xe}$  at 15 mT, respectively, were used. To reduce electrostatic noise, the RF coils were housed in a box covered with a copper sheet (0.1 mm thick). Coronal images were acquired using a gradient-echo imaging pulse sequence, with 32 phase encodes, without slice-selection in a field-of-view of 8 cm for helium imaging and 20 cm for xenon imaging. Each phase encode step was acquired with either one breath (about 2 mL) of hyperpolarized  $^3\text{He}$  using a  $75^\circ$  flip angle, or hyperpolarized  $^{129}\text{Xe}$  using a  $60^\circ$  flip angle. MR data acquisition was synchronized to the breath-hold period of the ventilation cycle.

**Human imaging.** A dual-surface RF coil array of 10 inch diameter was tuned to  $^3\text{He}$ . One coil was placed anterior and one placed posterior to the chest. About 500 mL of  $^3\text{He}$ , polarized to  $\sim 5\%$ , was expanded into an inert gas bag (Jensen Inert Products, Coral Springs, FL, USA) and handed to a healthy volunteer within the MRI magnet. Coronal images were acquired during a breath-hold of 10 s using a

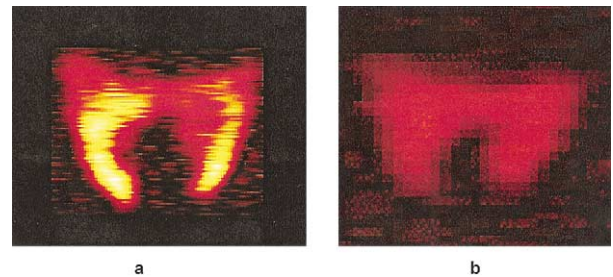


Fig. 1. Hyperpolarized (a)  $^3\text{He}$  image and (b)  $^{129}\text{Xe}$  image of the lungs in rats at very low magnetic field of  $B_0 = 15$  mT.

gradient-echo imaging pulse sequence, with 32 phase encodes and a flip angle of  $25^\circ$ . No slice-selection was employed and the field-of-view was 60 cm. The subject's left arm was positioned above the head for better accommodation within the bore of the MRI scanner. All imaging experiments were approved by the Human Research Committee at the Brigham and Women's Hospital.

## 3. Results

Fig. 1a depicts a gradient-echo hyperpolarized  $^3\text{He}$  image of the lungs of a live rat shown in coronal view during a breath-hold. This is the first VLF hyperpolarized noble gas image of a living animal. The left and right lungs are clearly seen, the heart indicated by the expected signal void. Since there is no slice selection, the image intensity does not closely correspond to the gas density, but even so, the edges are rather well defined. These images were obtained by lowering the field of an obsolescent whole-body superconducting magnet from its normal value of 1.5 T, down to 15 mT while a resistive solenoid magnet of suitable field homogeneity is being built and tested. Fig. 1b displays a coronal view of the lungs from a rat breathing hyperpolarized  $^{129}\text{Xe}$ . Although the image shows some lung structure and both lobes of the lung can clearly be seen, the signal-to-noise-ratio (SNR) is lower than in the  $^3\text{He}$  image. In typical  $^{129}\text{Xe}$  images the signal level is lower than in  $^3\text{He}$  images, both because the gyromagnetic ratio of  $^{129}\text{Xe}$  is 2.8 times smaller than that of  $^3\text{He}$ , and because the attainable level of polarization is generally lower. The polarization levels of Fig. 1 were modest, about 5%, while levels of  $\sim 50\%$  for  $^3\text{He}$  and  $\sim 20\%$  for  $^{129}\text{Xe}$  are presently achievable. Finally, Fig. 2 shows the first human VLF hyperpolarized noble gas image, of the lungs of a healthy subject inhaling  $^3\text{He}$ , demonstrating the potential of VLF HP gas MRI.

## 4. Discussion

In Fig. 2, while both lobes of the lung can be seen, the 10-inch diameter surface coil used for this image results in incomplete coverage of the lungs with an obvious lack of

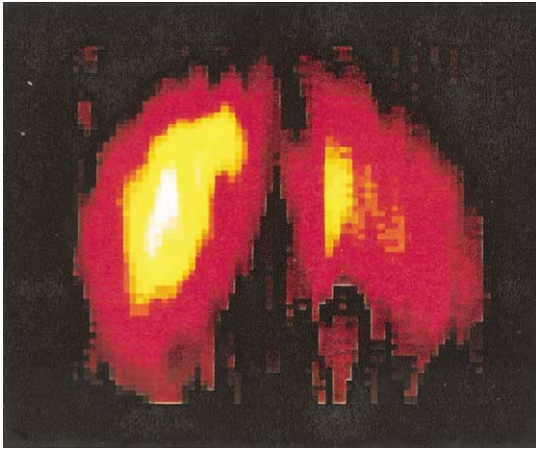


Fig. 2. Very low-field hyperpolarized  $^3\text{He}$  image of the human lungs. The position of the subject, together with the presence of the heart, contributed to an asymmetric appearance of the lobes of the lung.

signal from the apex and base. This will be remedied by larger imaging coils in saddle and bird-cage geometries currently under construction. The mediocre SNR in Fig. 2 is a consequence of *i*) poorly shielded external noise and *ii*) the noise from the coil and front-end electronics. Shielding of low frequency electromagnetic interference is a major problem in VLF MR experiments [17]. The scanner used in these experiments has shielding and filters optimized to minimize interference at the 66 MHz resonance frequency of protons at 1.5 T—hence they are quite ineffective in the 100–500 kHz range in which the resonance frequencies of  $^{129}\text{Xe}$  and  $^3\text{He}$  lie at 15 mT. We have made first order corrections to improve shielding, by shifting the roll-off frequencies of the low-pass filters on the wires entering the room. The other major noise source is the RF pickup-coil and front end. This noise can be minimized, unlike the noise in high-field MRI, where the dominant source is the biologic sample, which cannot be significantly modified.

In conventional MR applications, the advantages in increasing the strength of the magnetic field,  $B_0$ , accrue from the consequent increase in equilibrium magnetization and the increase in the energy of the transition, resulting in the signal scaling as  $B_0^2$ . In MRI the two significant sources of noise are *i*) the biologic sample, and *ii*) the coil and associated circuitry. Coil noise *emf* goes as  $\omega^{1/4}$  above  $\sim 1$  MHz, due to the skin-depth effect, but this weak dependence can be ignored at our very low frequencies. The noise *emf* from the sample goes as  $\omega$  (*i.e.*, as  $B_0$ ) and dominates over the Johnson noise from the coil at high-field, especially for large, coil-filling samples [18]. Thus, in conventional MRI, in the sample-noise dominated high-field regime, the SNR goes as  $B_0$ , and in the coil-noise dominated low field regime, the SNR goes as  $B_0^2$ , ignoring the small skin-depth effect. This traditional analysis would indicate rather dismal prospects for conventional MRI at very low fields.

In HP gas MRI, however, the signal scales with  $B_0$ , and not  $B_0^2$ , since the polarization is determined by the hyperpolarization technique, and is therefore independent of the

static magnetic field. Hence in combination with coil-noise, the SNR is independent of  $B_0$  at high field, and scales simply with  $B_0$  at low field. Since the  $\text{SNR}(\text{HP})/\text{SNR}(\text{water})$  ratio scales as  $1/B_0$ , HP gas MRI has a decisive advantage over conventional MRI at VLF. Wong *et al.* have argued that  $\text{SNR}(\text{HP})$  can be four orders of magnitude greater than  $\text{SNR}(\text{water})$  at 2 mT (20 G) [19]. Furthermore, since the source of noise at low field is the coil and associated electronics, cryogenic techniques can be used with profit. Superconducting coils with unloaded  $Q$ 's of  $>50,000$  [20] are an extravagance at high-field: especially with large coils and samples, the loading greatly reduces the  $Q$ , and, furthermore, the sample noise dominates. Sample noise and sample loading are almost negligible at VLF, especially with small coils. The use of high temperature superconducting (HTS) RF coils for small regions of interest can significantly improve the coil-noise limiting SNR. An increase in the SNR of MR images by a factor of 2 has been achieved at high-field (1.5 T), and by  $\sim 3.5$  at low- and intermediate-field strengths (0.2 T and 0.5 T) [21]. At VLF, an improvement in the SNR by a factor  $>10$  is not unreasonable, and can be used to improve speed and resolution. HTS material can nowadays be fashioned into coils operating at temperatures  $>77$  K, cooled with liquid nitrogen or liquid helium evaporate. We are currently examining HTS coils for our next generation system.

HP  $^3\text{He}$  MRI can visualize ventilation defects with a high sensitivity and is proving to be diagnostically useful in patients with various forms of pulmonary disease.  $^3\text{He}$  MR spectroscopy, localized by means of surface RF coils or volume selective gradients, produces large signals at very low-field, making possible regional measurements of the  $^3\text{He}$  longitudinal relaxation time,  $T_1$ , which can provide a local measure of the oxygen distribution in the lungs [22]. The solubility of  $^{129}\text{Xe}$  in blood and tissue opens up the possibility of monitoring blood-flow and cardiac and brain function [1,12]. Thus both gases should find significant uses in VLF MRI.

MRI at VLF will have reduced imaging distortions and spectral line broadening caused by heterogeneous magnetic susceptibilities, which is particularly advantageous for MRI in heterogeneous samples such as the lung [23,24]. Another important benefit is the extended  $T_2^*$ . We measured the  $T_2^*$  to be  $\sim 100$  ms for hyperpolarized gases in the lungs of living rats, similar to results reported in excised rat lungs [19]. Wong *et al.* and others have argued that the achievable imaging resolution for hyperpolarized gas imaging of the lung at VLF is limited by the diffusion of a gas, at both high and low-fields, to  $\sim 100$   $\mu\text{m}$  [19], adequate for most clinical studies. Finally, the relative field homogeneity requirements at VLF are less stringent because the image-encoding gradients ( $\sim 1$  Gauss/cm) are far greater in proportion to  $B_0$  than they are at high-field. A high-field, high homogeneity magnet, together with its special site housing and shielding is expensive. Resistive wire-wound solenoid magnets can easily and inexpensively be built [19,25,26] to fields of

10–20 mT (100–200 Gauss), and sited near other equipment with little shielding.

## 5. Conclusions

We have presented the first *in vivo* VLF HP gas MRI images of the lung gas-space in humans and in rats breathing hyperpolarized  $^3\text{He}$  and  $^{129}\text{Xe}$  at a field of 150 Gauss (15 mT). While preliminary, the analysis of the SNR and techniques available provide a clear pathway to sufficient resolution and high SNR while maintaining the ease and portability of MR at very low static fields. We envision portable VLF HP gas MRI on van-based imagers, on space-based platforms, and at sufficiently low field, MRI may even be offered to patients with metallic prostheses or implanted electronic equipment (*e.g.*, pacemakers), who have hitherto been denied the benefits of this imaging modality.

## Acknowledgments

We thank Ralph Hashoian, Chih-Liang Chin, Gabriel Gomez, Jamie McKendry, and Alexandra Rockefeller for assistance with MR system components. This work was supported by grants from the National Institutes of Health (R01-HL57563), the National Science Foundation (BES-9617342), the Whitaker Foundation (RG 95-0192), and the National Aeronautics and Space Administration (NAG9-1041).

## References

- [1] Albert M, Cates G, Driehuys B, Happer W, Saam B, Springer CS, Wishnia A. Biological magnetic resonance imaging using laser-polarized  $^{129}\text{Xe}$ . *Nature* 1994;370:199–201.
- [2] Kauczor HU, Hofmann D, Kreitner KF, Nilgens H, Surkau R, Heil W, Roberts T, Pothast A, Knopp MV, Otten EW, Thelen M. Normal and abnormal pulmonary ventilation: Visualization at hyperpolarized He-3. *MR Imaging Radiology* 1996;201:564–8.
- [3] de Lange EE, Mugler JP, Brookeman JR, Knight-Scott J, Truwit JD, Teates CD, Daniel TM, Bogorad PL, Cates GD. Lung Air Spaces: MR Imaging Evaluation with Hyperpolarized  $^3\text{He}$  Gas. *Radiology* 1999;210:851–7.
- [4] Donnelly LF, MacFall JR, McAdams HP, Majure JM, Smith J, Frush DP, Bogard P, Charles HC, Ravin CE. Cystic Fibrosis: Combined hyperpolarized  $^3\text{He}$ -enhanced and conventional proton MR imaging in the lung—preliminary observations; *Radiology* 1999;212:885–9.
- [5] Altes TA, Powers PL, Knight-Scott J, Rakes G, Platts-Mills TA, de Lange EE, Alford BA, Mugler JP, Brookeman JR. Hyperpolarized  $^3\text{He}$  MR lung ventilation imaging in asthmatics: preliminary findings. *J Magn Reson Imaging* 2001;13:378–84.
- [6] McAdams H, Palmer S, Donnelly L, Charles H, Tapson V, MacFall J. Hyperpolarized  $^3\text{He}$ -enhanced MR imaging of lung transplant recipients: Preliminary results. *AJR* 1999;173:955–9.
- [7] Happer W, Miron E, Schaefer S, Schreiber D, van Wijngaarden WA, Zeng X. Polarization of the nuclear spins of noble-gas atoms by spin exchange with optically pumped alkali-metal atoms. *Phys Rev A* 1984;29:3092–110.
- [8] Mugler JP, Driehuys B, Brookeman JR, Cates GD, Berr SS, Bryant RG, Daniel TM, de Lange EE, Downs JH, Erickson CJ, Happer W, Hinton DP, Kassel NF, Maier T, Phillips D, Saam BT, Sauer KL, Wagshul ME. MR imaging and spectroscopy using hyperpolarized  $^{129}\text{Xe}$  gas: Preliminary human results. *Magn Reson Med* 1997;37:809–15.
- [9] Moller HE, Chawla MS, Chen XJ, Driehuys B, Hasson KC, Hedlund LW, Wheeler CT, Johnson GA. Magnetic resonance angiography with hyperpolarized  $^{129}\text{Xe}$  dissolved in lipid emulsion. *Magn Reson Med* 1999;41:1058–64.
- [10] Sakai K, Bilek AM, Oteiza E, Walsworth RL, Balamore D, Jolesz FA, Albert MS. Temporal dynamics of hyperpolarized  $^{129}\text{Xe}$  resonances in living rats. *J Magn Reson Series B* 1996;111:300–4.
- [11] Swanson SD, Rosen MS, Agranoff BW, Coulter KP, Welsh RC, Chupp TE. Brain MRI with laser-polarized  $^{129}\text{Xe}$ . *Magn Reson Med* 1997;38:695–8.
- [12] Swanson SD, Rosen MS, Coulter KP, Welsh RC, Chupp TE. Distribution and dynamics of laser-polarized  $^{129}\text{Xe}$  magnetization in vivo. *Magn Reson Med* 1999;42:1137–45.
- [13] Black RD, Middleton HL, Cates GD, Cofer GP, Driehuys B, Happer W, Hedlund LW, Johnson GA, Shattuck MD, Swartz JC. In vivo He-3 MR images of guinea pig lungs. *Radiology* 1996;199:867–70.
- [14] Darrasse L, Guillot G, Nacher PJ, Tastevin G. Low-field  $^3\text{He}$  nuclear magnetic resonance in human lungs. *CR Acad Sci Paris* 1997;324:691–700.
- [15] Augustine MP, Annjoe WF, Yarger JL, Tomaselli M, Pines A. Low field magnetic resonance images of polarized noble gases obtained with a dc superconducting quantum interference device. *Appl Phys Lett* 1998;72:1908–10.
- [16] Tseng CH, Wong GP, Pomeroy VR, Mair RW, Hinton DP, Hoffmann D, Stoner RE, Hersman FW, Cory DG, Walsworth RL. Low-field MRI of laser polarized noble gas. *Phys Rev Lett* 1998;81:3785–8.
- [17] Planinsic G. Shielding of low-frequency magnetic interference in weak-field MRI by a single-layer cylindrical coil. *J Magn Reson* 1997;126:30–8.
- [18] Hoult DI, Richards RE. The signal-to-noise of the nuclear magnetic resonance experiment. *J Magn Reson* 1976;24:71–85.
- [19] Wong GP, Tseng CH, Pomeroy VR, Mair RW, Hinton DP, Hoffmann D, Stoner RE, Hersman FW, Cory DG, Walsworth RL. A system for low field imaging of laser-polarized noble gas. *J Magn Reson* 1999;141:217–27.
- [20] Black RD, Early TA, Roemer PB, Mueller OM, Mogro-Campero A, Turner LG, Johnson GA. A high-temperature superconducting receiver for nuclear magnetic resonance microscopy. *Science* 1993;259:793–5.
- [21] Ma QY., Gao E., Miller JR., Xu H., Chan KC., Wong KK., Yang ES., Kacher DF., Young GS., Jolesz FA., Face DW., Kountz DJ. Superconducting MR surface coils for human imaging. *Proceedings of the International Society of Magnetic Resonance in Medicine, 7th Scientific Meeting, Philadelphia* 1999, p. 171.
- [22] Deninger AJ, Eberle B, Ebert M, Grossmann T, Heil W, Kauczor H-U, Lauer L, Markstaller K, Otten E, Schmiedeskamp J, Schreiber W, Surkau R, Thelen M, Weiler N. Quantification of regional intrapulmonary oxygen partial pressure evolution during apnea by  $^3\text{He}$  MRI. *J Magn Reson* 1999;141:207–16.
- [23] Bergin CJ, Glover GH, Pauly JM. Lung parenchyma: Magnetic susceptibility in MR imaging. *Radiology* 1991;180:845–8.
- [24] Macovski A, Conolly S. Novel approaches to low-cost MRI. *Magn Reson Med* 1993;30:221–30.
- [25] Hanson RJ, Pipkin FM. Magnetically shielded solenoid with field of high homogeneity. *Rev Sci Inst* 1965;36:179–88.
- [26] Morgan P, Conolly S, Scott G, Macovski A. A readout magnet for prepolarized MRI. *Magn Reson Med* 1996;36:527–36.
- [27] Venkatesh A, Zhao L, Pausak T, Ward C, Jolesz FA, Albert MS. Hyperpolarized gas imaging using a simple programmable gas delivery system. *Eur Radiol* 1999;9:B34.